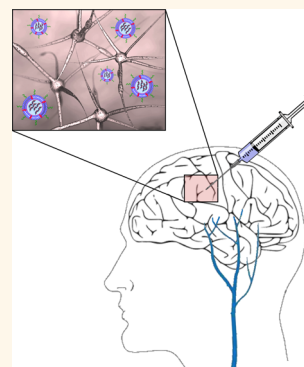


Localized RNAi Therapeutics of Chemoresistant Grade IV Glioma Using Hyaluronan-Grafted Lipid-Based Nanoparticles

Zvi R. Cohen,^{†,||} Srinivas Ramishetti,^{*,§,||} Naama Peshes-Yaloz,^{†,||} Meir Goldsmith,^{*,§,||} Anton Wohl,[†] Zion Zibly,[†] and Dan Peer^{*,§,||}

[†]Department of Neurosurgery, Sheba Medical Center, Ramat Gan, Israel and [‡]Laboratory of NanoMedicine, Department of Cell Research and Immunology, George S. Wise Faculty of Life Sciences; [§]Department of Materials Sciences and Engineering, Faculty of Engineering; [⊥]Center for Nanoscience and Nanotechnology Tel Aviv University, Tel Aviv 69978, Israel. ^{||}These authors contributed equally to this work.

ABSTRACT Glioblastoma multiforme (GBM) is one of the most infiltrating, aggressive, and poorly treated brain tumors. Progress in genomics and proteomics has paved the way for identifying potential therapeutic targets for treating GBM, yet the vast majority of these leading drug candidates for the treatment of GBM are ineffective, mainly due to restricted passages across the blood–brain barrier. Nanoparticles have been emerged as a promising platform to treat different types of tumors due to their ability to transport drugs to target sites while minimizing adverse effects. Herein, we devised a localized strategy to deliver RNA interference (RNAi) directly to the GBM site using hyaluronan (HA)-grafted lipid-based nanoparticles (LNPs). These LNPs having an ionized lipid were previously shown to be highly effective in delivering small interfering RNAs (siRNAs) into various cell types. LNP's surface was functionalized with hyaluronan (HA), a naturally occurring glycosaminoglycan that specifically binds the CD44 receptor expressed on GBM cells. We found that HA-LNPs can successfully bind to GBM cell lines and primary neurospheres of GBM patients. HA-LNPs loaded with Polo-Like Kinase 1 (PLK1) siRNAs (siPLK1) dramatically reduced the expression of PLK1 mRNA and cumulated in cell death even under shear flow that simulate the flow of the cerebrospinal fluid compared with control groups. Next, a human GBM U87MG orthotopic xenograft model was established by intracranial injection of U87MG cells into nude mice. Convection of Cy3-siRNA entrapped in HA-LNPs was performed, and specific Cy3 uptake was observed in U87MG cells. Moreover, convection of siPLK1 entrapped in HA-LNPs reduced mRNA levels by more than 80% and significantly prolonged survival of treated mice in the orthotopic model. Taken together, our results suggest that RNAi therapeutics could effectively be delivered in a localized manner with HA-coated LNPs and ultimately may become a therapeutic modality for GBM.



KEYWORDS: glioma · hyaluronan · lipid-based nanoparticles · RNAi

Many approaches have been used to treat high-grade glioblastoma multiforme (GBM); however, all of them have failed to improve prognostic and quality of life of patients suffering from this devastating disease. Several groups have reported survival benefits when extent of resection was used as a prognostic factor.^{1–3} The use of advanced technology in the operating room (OR) theater have led to more reports supporting aggressive surgical approach to maximize the extent of resection. A multicenter phase III trial⁴ comparing fluorescence guided microsurgery with conventional microsurgery of GBM showed a survival benefit in patients who underwent

complete tumor resection according to the assessment of residual contrast enhancement on postoperative magnetic resonance images (MRI). Recently, the use of intraoperative MRI guidance showed a benefit in terms of extent of resection compared to conventional microsurgical tumor resection.⁵ Besides the local control of the disease by complete removal, which may increase time to progression and survival in a subgroup of patients,¹ and in addition to the use of temozolomide and radiotherapy for patients with favorable methylation status,⁶ little progress has been made in the treatment of adult glioblastoma.

Several phase III clinical trials^{6,7} in the past decade have all failed to change the course

* Address correspondence to peer@tauex.tau.ac.il.

Received for review November 2, 2014 and accepted January 5, 2015.

Published online January 05, 2015
10.1021/nn506248s

© 2015 American Chemical Society

of the disease. The failure of gene therapy, brachytherapy, and convection enhanced delivery of toxins and chemotherapy in treating high-grade GBM have paved the way to other innovative approaches such as the use of nanotechnology.

The use of nanomedicine has emerged to elucidate the relationship of the physical and chemical properties (size, shape, surface chemistry, composition, and aggregation) of nanostructures with the ability to deliver therapeutic payloads effectively into tumor cells.^{8,9} Recently, the use of nanoparticles (NPs) has become a potential strategy for diagnosis and treatment of GBM,¹⁰ and several studies have shown that different drugs or their active metabolites entrapped in various types of lipid-based nanoparticles (LNPs) or polymeric nanoparticles such as PLGA may enhance the therapeutic benefit when treating GBM.^{11–15}

Hyaluronan (HA), a naturally occurring glycosaminoglycan, has been shown to play crucial roles in cell growth, embryonic development, healing processes, inflammation, and tumor development and progression.^{8,16} HA, the major ligand of the CD44 receptor overexpressed or constitutively expressed on many types of cancer cells, has been widely used by several groups for the past decade as a targeting moiety coated on the surface of different types of NPs.^{17–23} HA coating on the NPs' surface that were systemically administered into mice bearing different types of tumors have endowed these carriers with long circulation properties similar to polyethylene glycol (PEG) and shown to target these carriers into tumor cells in a CD44-dependent manner.^{18,22} Interestingly, only a few studies examined the interaction between CD44 and HA in the context of targeting capabilities with different MW of HA coated on the surface of LNPs.^{23,24}

Utilizing HA as a targeting moiety endow carriers with specificity to recognize only activated CD44 that can efficiently bind HA. Bachar *et al.*²⁵ have tested primary thyroid tumors and normal thyroid cells taken from the same patient in the OR and found that although CD44 expression in both healthy and cancerous thyroid was high, HA-coated LNPs clusters bound only to the cancerous cells and not to healthy cells in a highly selective manner.²⁵

Taken together, these results support the use of HA as a targeting moiety for activated CD44 expressed on cancer cells.

Pololike kinase 1 (PLK1), a serine/threonine-protein kinase, is an early trigger for G2/M transition during the cell cycle. PLK1 has been reported to play important roles in malignant transformation.²⁶ Investigation into the clinicopathological significance of PLK1 expression in GBM showed that the expression of PLK1 at the mRNA was significantly higher in glioma tissues than in corresponding normal brain tissues.²⁷ The expression of PLK1 mRNA was closely correlated with WHO grade, KPS, and tumor recurrence of glioma patients

($P = 0.022$, 0.030 , and 0.041 , respectively). Multivariate analysis showed that high PLK1 mRNA expression was a poor prognostic factor for GBM patients ($P = 0.028$).²⁸

We hypothesized that targeting PLK1 could serve as a novel therapeutic approach to kill chemoresistant GBM. Thus, we devised a novel strategy based on HA-coated LNPs to locally target high grade GBM and deliver PLK1-siRNAs (siPLK1) as a potential RNAi therapeutic to eradicate GBM.

RESULTS AND DISCUSSION

Wide Expression of CD44 on GBM Cell Lines and Primary Tumors. We examined the expression of CD44 in human GBM cell lines by flow cytometry and in primary glioma samples (excreted from GBM patients) by immunohistochemistry (Figure 1). Three representative GBM cell lines were used: T98G, U87MG, and U251 all have been reported to be resistant to chemotherapy treatment.²⁹ Pan anti-CD44 mAb was used to detect the expression of CD44 in all three-cell lines, and all have shown to have a high CD44 expression (Figure 1A). Next, we examined the expression of CD44 in primary glioma cells excreted from patients using immunohistochemistry. Representative stainings are shown in Figure 1B, and a list of patients samples with semiquantitative analysis of CD44 expression is depicted. The high expression of CD44 in both cell lines and primary glioma cells enable the use of the natural CD44 ligand, HA, as a targeting moiety coated on LNPs that can aid in cellular retention to and internalization into glioma cells.

Synthesis and Characterization of HA-Coated LNPs Entrapping siRNAs. LNPs containing siRNAs were prepared using a microfluidic micro mixture as previously reported with the inclusion of the ionized lipid Dlin-MC3-DMA³⁰ (see supplementary Figures 1 and 2, Supporting Information) and a small amount (0.5 mol %) of DSPE-PEG-NH₂ as detailed in the Methods. Next, in order to functionalize these LNPs containing siRNAs with HA, the carboxylic groups of HA (MW 5KDa) were activated by classical EDC/sulfo-NHS chemistry. HA (0.3 mg, 5×10^5 mmol) was dissolved in water followed by the addition of a carbodiimide, EDC (0.2 mg, 10×10^5 mmol), and sulfo-NHS (0.3 mg, 10×10^5 mmol). The reaction mixture was stirred gently by shaker for 2 h followed by addition of amine-functionalized nanoparticles at pH 7.8 (containing 0.03 mg of PEG-amine, 1×10^5 mmol) and stirring continued for additional 3 h at room temperature. The reaction mixture was dialyzed against PBS, pH 7.4 using a 12–14 kD cutoff membrane for 24 h to remove excess HA and cross-linkers.

A schematic illustration of the HA conjugation to LNPs is listed in Figure 2.

Typical size distribution of LNPs-NH₂ entrapping siRNAs were around 80 nm in diameter with a narrow size distribution as measured by dynamic light scattering and a mildly positive ζ potential (Figure 3A). Conjugating HA to LNPs increased the size distribution

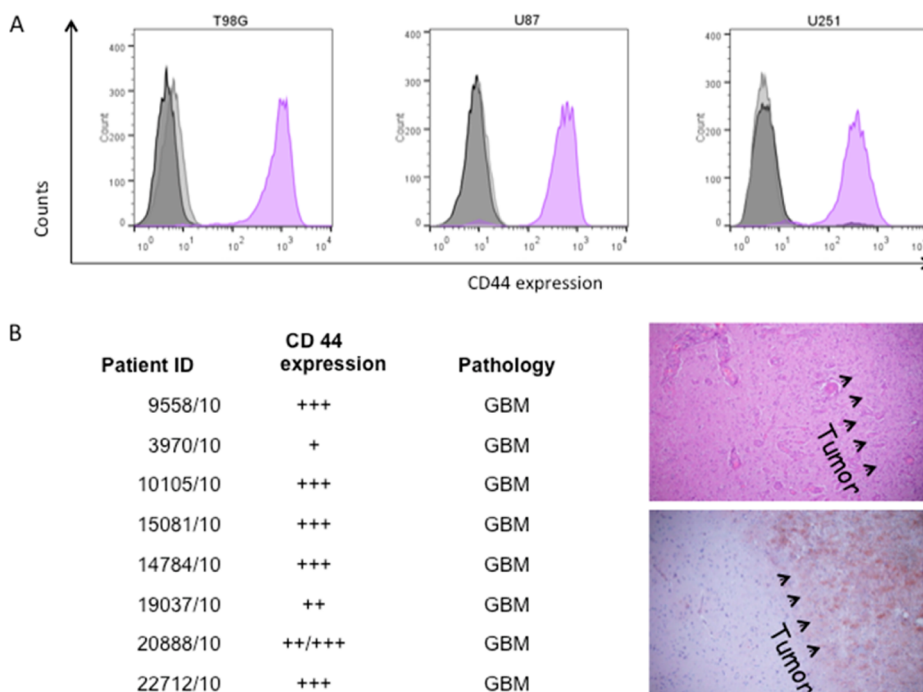


Figure 1. CD44 is highly expressed in GBM cell lines and primary glioma cells. (A) Representative histograms of CD44 expression in GBM cell lines. An anti pan-CD44 mAb was used to stained three different GBM cell lines: T98G, U87MG, and U251 (light gray, no stain; gray, isotype control mAb; purple, anti pan-CD44 mAb (clone IM7)). (B) CD44 expression in primary glioma samples excreted from patients using immunohistochemistry analysis as detailed in the Methods. Analysis score was based on CD44 scattering within the tumor site. This staining is semiquantitatively scored: + (positive), ++ (strongly positive), or +++ (very strongly positive).

Synthesis of HA-LNPs:

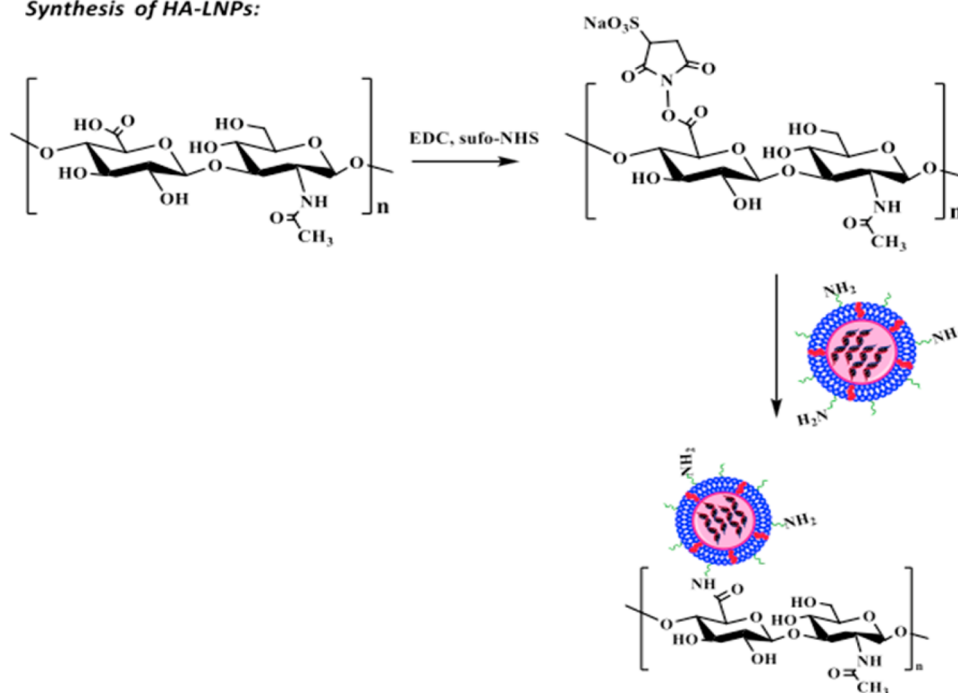


Figure 2. Schematic illustration of HA conjugation to LNPs-PEG-NH₂. HA (5KDa) is activated by classical amine coupling strategy (EDC and Sulfo-NHS) as detailed in the Methods. LNPs-PEG-NH₂ entrapping siRNAs using the microfluidic nanoassembly is then mixed and incubated with the activated HA. Purification of unbound HA is performed using extensive dialysis as detailed in the experimental section.

of the LNPs to about 100 nm in diameter and decreased the ζ potential to around -8 mV (Figure 3A). These findings are in good agreement with previously

reported studies showing increase in size distribution and decrease in ζ potential when HA was present on LNPs surface.^{24,22,23} The entrapment efficiency of

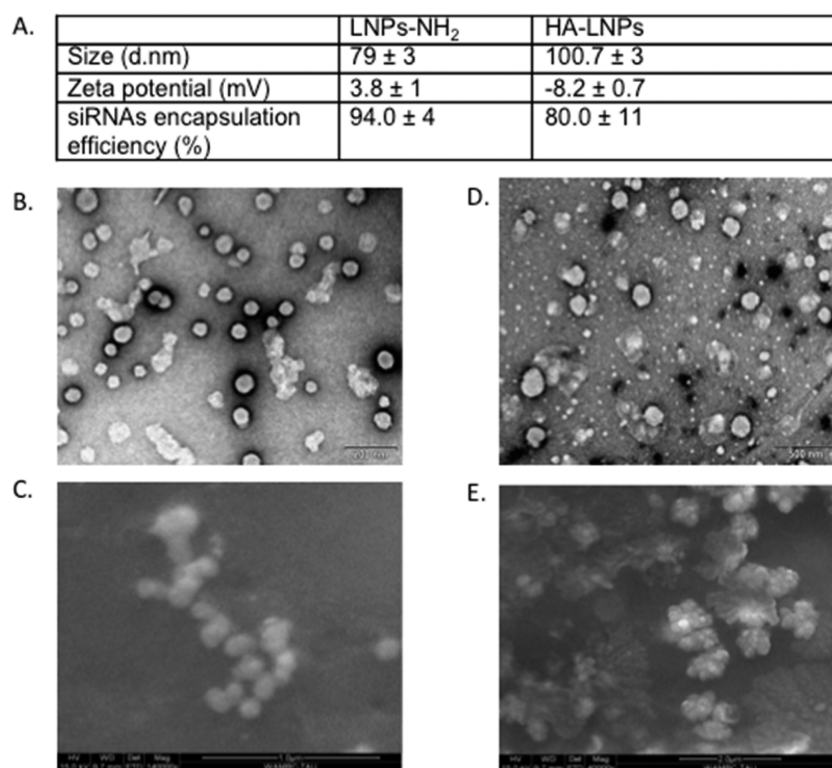


Figure 3. Physicochemical and structural characterization of HA-LNPs and LNPs-NH₂. (A) Size distribution and ζ potential are performed on a Malvern ζ sizer as detailed in the Methods. Entrapment of siRNAs is measured using Ribogreen assay as detailed in the Methods. (B and D) TEM analysis of LNPs-NH₂ and HA-LNPs, respectively. Bar scale: 200 nm. (C and E) SEM analysis of LNPs-NH₂ and HA-LNPs, respectively. Bar scale: 1 μ m. Methods and instrumentation are detailed in the Methods. LNPs-NH₂ were found to have globular shapes and round surfaces whereas HA-LNPs exhibit a flower-like shape on the particles.

siRNAs was \sim 94% for LNPs-NH₂ and \sim 80% for HA-LNPs assayed by a ribogreen assay as previously reported (Figure 3A).³¹ The ultrastructure of HA-LNPs and LNPs-NH₂ was investigated using transmission electron microscopy (TEM) and scanning electron microscopy (SEM) (Figure 3B–E). LNPs-NH₂ were found to have globular shapes in TEM (Figure 3B) and SEM (Figure 3C) with typical diameters of \sim 80–90 nm. HA-LNPs also had globular shapes in TEM (Figure 3D) with flower-like structures found in SEM (Figure 3E). These particles had larger diameters (above 100 nm in diameter in average).

HA-LNPs Bind to Glioma Cells. We next investigated if HA-LNPs can specifically bind to glioma cells. Both types of particles entrapped Cy5-siRNAs that were used as a sensitive marker. HA-LNPs bound to U87MG cells (Figure 4A) and primary GBM from GBM patients (Figure 4B). The control particles without the targeting ligand, LNPs-NH₂, did not bind U87MG or the primary glioma patient sample. These results are in good agreement to other nanoscale delivery platforms that utilized HA as their targeting moiety toward cells expressing CD44.^{17,18,22–24,32} Moreover, a study conducted on primary cells from patients with head and neck cancers found that HA binds with high affinity only to thyroid cancer cells but not normal thyroid cells from the same patient.²⁵ In another study, when cells expressing CD44

were blocked with a mAb against pan-CD44, HA was not able to bind the cells.²¹ Taken together, these results support the hypothesis that utilizing HA as a targeting moiety coated on the surface of nanoscale drug delivery systems provide selective targeting to cells expressing an activated form of CD44 (or clustered receptors) and might be used for active cellular targeting.

PLK1 Induce Cell Death in Glioma Cells. GBM cells are known to be resistant to chemotherapy.³³ In order to verify resistance of U87MG cells to chemotherapy we tested two classical chemotherapeutic agents (doxorubicin and BCNU) at different doses. Both confirmed the inherent resistance of U87MG (Supplementary Figure 3, Supporting Information). Thus, the use of a sequence specific cell cycle inhibitors in the form of an siRNA is expected to bypass this resistance mechanism since large molecules are not effluxed out from cells by extrusion pumps.^{33,34} We entrapped siPLK1 or control siRNA (siLuciferase; siLuci) in HA-LNPs and in the control particles (LNPs-NH₂) lacking the targeting ligand. HA is expected to retain the particles at the cell surface or inside the cells as binding of HA to CD44 (in the case of cancer cells) have a low K_d as we previously shown.^{22,24} The experiment was done under shear flow conditions as previously detailed³⁵ in order to simulate the cerebrospinal fluid

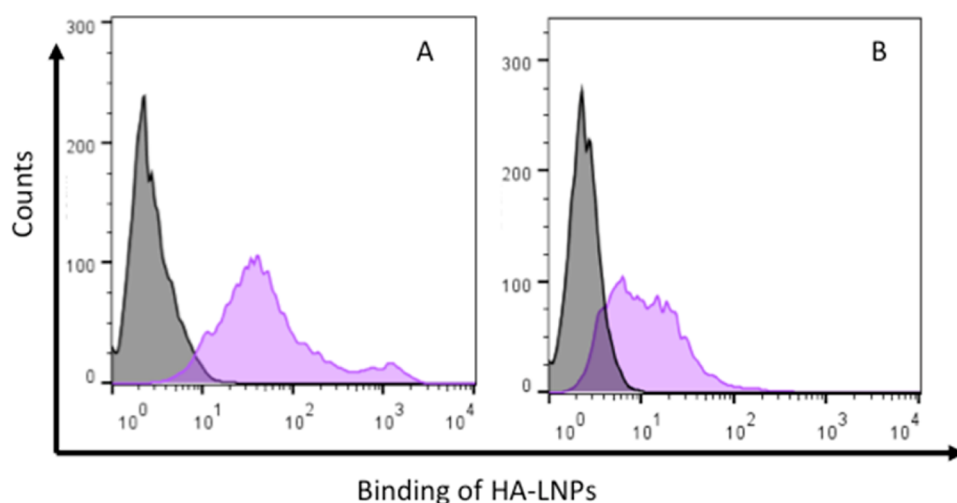


Figure 4. HA-LNPs bind specifically to glioma cells. (A) Representative histograms are shown. HA-LNPs (purple curve) specifically bind to GBM cell line (U87MG cells) whereas LNPs-NH₂ (gray curve) did not bind to the GBM glioma cell line. (B) HA-LNPs (purple curve) bound to patient sample whereas the control particles, LNPs-NH₂ (gray curve), did not bind the cells.

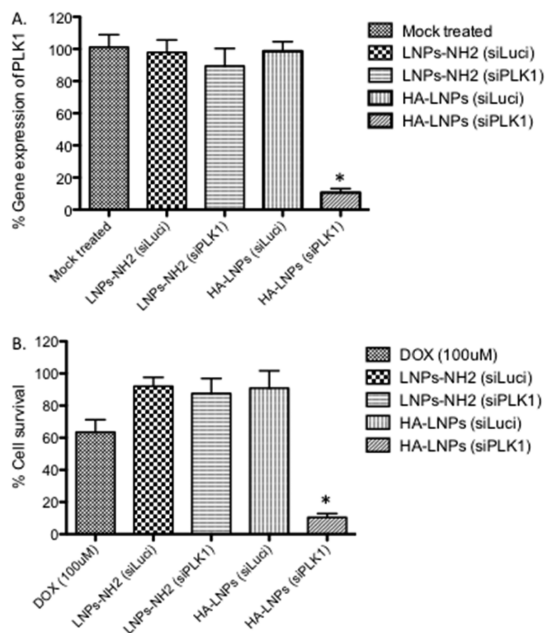


Figure 5. PLK1 induce specific cell death in glioma cells. (A) PLK1 gene expression was quantifying using QPCR as detailed in the Methods. U87MG cells were incubated with HA-LNPs or LNPs-NH₂ with either siLuci or siPLK1 under shear flow conditions to simulate CSF flow. A robust knock-down was observed in the siPLK1 treatment when delivered via HA-LNPs. (B) XTT cell survival assay was performed on cells treated with the same types of treatments as listed in (A). Doxorubicin (DOX), a known chemotherapy, was used as a positive control. * $p < 0.001$.

(CSF) flow for 10 min followed by incubation in static condition with fresh media. At 72 h post transfection, cells were analyzed for mRNA levels of PLK1.

HA-coated LNPs induced a robust gene silencing under shear flow both at the mRNA and PLK1 protein level (Figure 5A and Supplementary Figure 4, Supporting Information). PLK1 protein was silenced for 96 h and recovery of the protein level was observed at 144 h

post transfection (Supplementary Figure 4, Supporting Information). This silencing effect was specific since HA-coated LNPs with siLuci did not reduce the expression of PLK1 mRNA. In addition, the robust silencing observed with siPLK1 delivered via HA-LNPs was translated to effective cell death (Figure 5B). The control particles (LNPs-NH₂) did not reduce mRNA levels of PLK1 when siPLK1 or siLuci were applied, nor did they induce cell death. This implies that the HA coating on the LNPs surface bind with high affinity to CD44 expressed on the GBM cells even under shear flow and that the internalization process is fast and efficient. These results are in good agreement with our previous confocal microscopy analysis that shows in ovarian cancers and in melanoma (all expressing high levels of CD44) an efficient and fast internalization of HA-coated nanoparticles.^{22,23}

U87MG Orthotopic Xenograft Model Establishment. Next, we utilized human U87MG cells to generate an orthotopic xenograft model in athymic BALB/c *nu/nu* mice. This is a well-established model for studying the growth, biology, and treatment of human gliomas.³⁶ We injected 3- μ L suspension of 5×10^5 U87MG cells into each animal as detailed in the Methods. Histological analysis was performed at day 12 post-inoculation, and a representative histology is presented in Figure 6.

Cy3-siRNAs Delivered via HA-LNPs Are Taken up by U87MG Cells *in Vivo*. Next, we administered 3 μ L of 0.2 mg/kg body Cy3-siRNAs via HA-LNPs or via LNP-NH₂ directly into the tumor vicinity at day 20 from tumor inoculation (see the Methods for more details) and sacrificed the mice ($n = 6$), 3, 6, and 24 h post HA-LNPs administration. Brain were sectioned and immediately taken into confocal microscopy analysis to identify the distribution of the Cy3-siRNAs within the tumor at different time points. Representative data are presented in Figure 7.

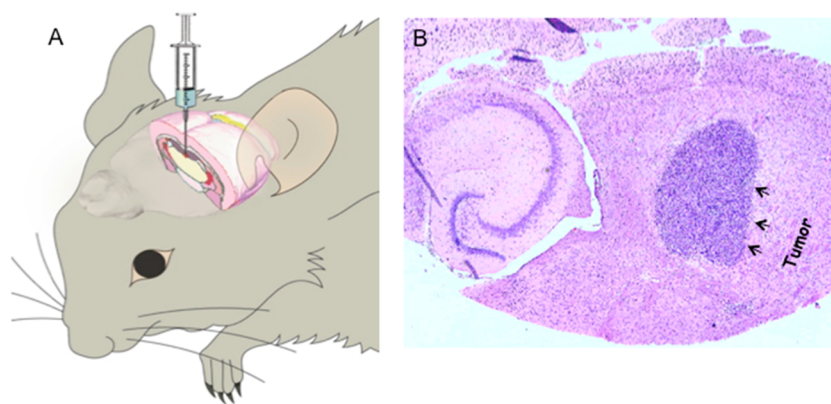


Figure 6. Orthotopic GBM model. (A) Schematic illustration of stereotactic implantation of the U87MG cells. (B) Representative histological analysis using H&E staining was conducted to evaluate tumor size and location 12 days post tumor inoculation.

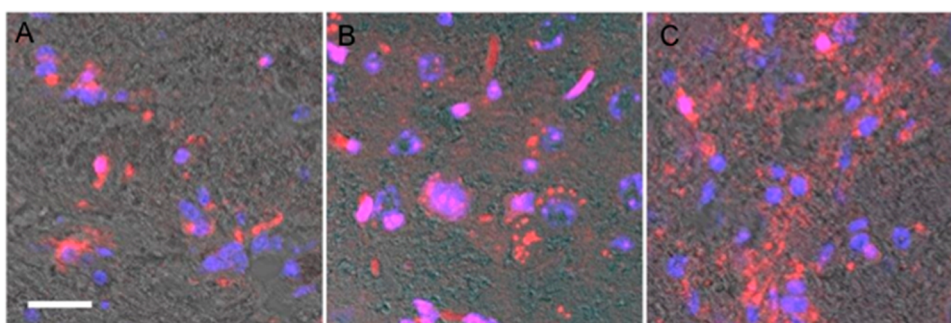


Figure 7. Cy3-siRNAs are taken up by U87MG cells. Representative confocal microscopy images are presented. HA-LNPs were injected into tumor site as detailed in the Methods. Three hours (A), 6 h (B), and 24 h (C) after LNPs administration, animals were sacrificed and the Cy3-siRNA (red) location was detected using confocal microscopy analysis. DAPI (blue) was used for nuclear staining. Bar scale, 50 μm .

Detection of Cy3 signal was observed only in HA-LNPs treated mice in all sections (Figure 7) and increased with time from 3 to 6 to 24 h post-administration (compare Figure 7A–C). We attribute this result to the specific binding of HA to CD44 expressed on U87MG cells. When administered with LNPs-NH₂ we could not detect any Cy3 signal in the tumor tissue (data not shown). This result is in good agreement with the result we obtained when LNPs-NH₂ did not adhere to U87MG cells under shear flow (Figure 5) since we have not observed silencing of PLK1 or cell death associated with their incubation with the cells under shear flow. We speculate that shear flow by the CSF may cause LNPs-NH₂ not to adhere to the U87MG cells.

Silencing of PLK1 in U87MG Cells Prolongs the Survival of GBM-Bearing Mice. We next utilized the GBM orthotopic model to test *in vivo* silencing of PLK1 upon 2 local administrations (0.5 mg/kg body each) at day 20 and 22 of tumor inoculation. In order to identify the tumor cells from other types of cells in the brain, tumor tissue was taken out, a single cell suspension was made (see the Methods), and the cells were incubated with a surface marker expressed on U87MG cells (CD44v6).³⁷ An antihuman CD44v6-FITC (non-cross-reactive with

mice) was incubated on ice for 30 min and then washed twice and subjected to FACS sorting as detailed in the Methods. FACS (FACSAria III, BD)-sorted cells were analyzed for PLK1 mRNA levels using QPCR. A robust knockdown of 80% was observed in U87MG CD44v6⁺ cells treated with siPLK1 that was delivered *via* HA-LNPs (Figure 8A). We have not observed any silencing with siLuci as expected. Since we have not seen any delivery of Cy3-siRNAs with the LNPs-NH₂ strategy we did not include this delivery system in this experimental setting.

Next, we isolated primary mouse cells from the brain (see the Methods), and FACS sorted these cells using an antimouse CD11b mAb in order to obtain mouse microglia cells. These cells might be involved in a potential local inflammatory response when siRNAs are delivered.³⁸ We incubated these cells with siPLK1 entrapped in HA-LNPs at two doses (0.05 and 0.5 mg/kg siRNA) and probed for TNF- α and IL-6 levels 6 h post incubation with the primary cells. LPS was used as a positive control. We have not observed any induction of the proinflammatory cytokines in the low concentration and a very mild induction in the higher concentration (Supplementary Figure 5, Methods). These results support the hypothesis that HA-LNPs

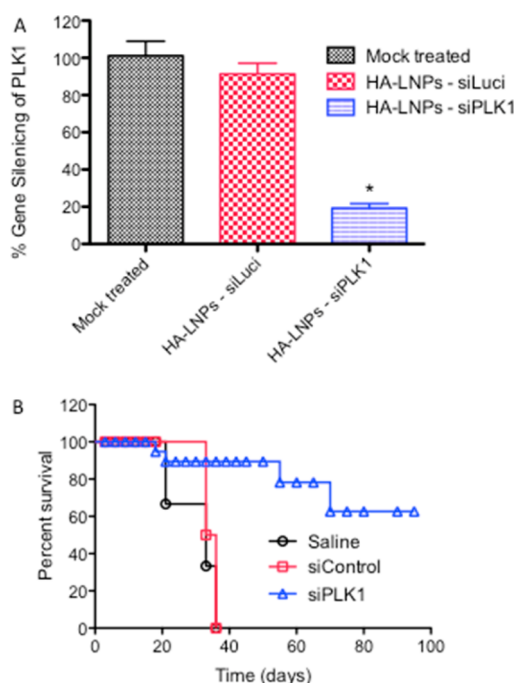


Figure 8. Therapeutic gene silencing prolongs the survival of GBM-bearing mice. (A) Robust *in vivo* gene silencing in siPLK1 treated mice is shown ($n = 10$ mice/group). Animals were treated twice as detailed in the Methods. Tumor cells were FACS sorted *via* a surface marker, and PLK1 mRNA level was quantified using QPCR. * $p < 0.001$. (B) Kaplan–Meier survival analysis of GBM-bearing orthotopic U87MG cells ($n = 10$ /group) treated with siControl (siLuciferase), siPLK1, or saline. Overall, four administrations were given at days 7 and 9 post tumor inoculation and then at days 20 and 22 post tumor inoculation.

protect siRNA in a very efficient manner and do not trigger a proinflammatory response even when directly interacting with CD11b⁺ cells.

It has been shown that robust silencing of PLK1 induced tumor regression in different tumors implanted in nude or SCID mice.^{26,39} We used the orthotopic GBM model to examine the effect on survival of the mice (Figure 8B). We administered four times locally into the GBM tumor site 3 μ L (per administration) of 0.5 mg/kg body of siPLK1 or siLuci at days 7 and 9 post-tumor inoculation and again at days 20 and 22 post tumor inoculation. It was reported that the median survival of mice (mock treated) in this model range from 24 to 30 days post-tumor inoculation.³⁶ In our hands, the median survival of Mock-treated mice was 33 days. Mice receiving four administrations of siLuci in HA-LNPs had a median survival of 34.5 days, and those receiving siPLK1 had prolonged survival with a remarkable 60% survival at day 95 post-tumor inoculation according to Kaplan–Meier survival analysis ($p = 0.0012$, between the siPLK1- and siLuci-treated group). This is the longest ever reported survival of mice in this orthotopic GBM model. In addition, this is the first time therapeutic siRNAs are being used in localized treatment to achieve therapeutic benefit in an orthotopic model of GBM.

Our findings with siPLK1-loaded HA-LNPs may be expanded for additional targets, using payloads that may yield a more potent effect. We assume that an optimal selection of the target genes should take into consideration the specific GBM subtype, as different subtypes present different genetic profile. Subtype specific payloads could thus be targeted toward Notch pathway or PDGFRA for proneural GBMs,² EGFRvIII for Classic GBM or PD-L1,³ and RelB (an oncogenic driver of tumor growth and invasion²) for mesenchymal GBM. In addition, treatment could also be directed toward glioma-like stem cells (GSCs), which are radio-resistant and chemo-resistant (leading to tumor recurrence), by using siRNA against STAT3 or SOX2.⁴⁰ Other potential therapeutic targets include the tumor microenvironment, which was shown to play an important role in tumor progression, stem cells maintenance, and therapy resistance.^{41,42} RNAi targeted for the microenvironment include siRNAs for immunosuppression (siRNA for PD-L1 and IDO)⁴³ or angiogenesis.⁴⁴

GBM is a complex and genetically unstable tumor characterized by a multitude of chromosomal gains and losses, gene mutations and amplifications, epigenetic dysregulation, and aberrant post-translational modifications. We assume that in order to effectively overcome GBM resistance, multitargeting payload should be used. To that end, combinational treatment with multiple siRNAs simultaneously or miRs might provide a clinical therapeutic benefit. HA-LNPs delivery strategy can potentially carry sufficient amounts of RNAi payloads and thus has the capacity to load combinations of RNAi to silence several pathways simultaneously. Examples include silencing for growth factors (such as EGFR, PDGFR), inhibition of angiogenesis pathways (such as VEGF, Integrins), or inhibition of intracellular signaling pathways (such as PI3K/AKT/mTOR or Ras/Raf/MAPK). Other combinations will be directed toward cancer stem cells targeting CXCR4 with VEGF, PDK1 with CHK1, and EGFR with PDGFR. Alternatively, a single miRNA that may regulate number of target genes and suppress and/or silence cellular pathway(s) could serve as the desired payload.⁴⁵

HA-LNPs loaded with RNAi could also be combined with conventional treatment to increase tumor susceptibility to chemotherapy and irradiation, namely, targeting genes like MGMT, Cx43, Her1/EGF-R,⁴⁶ VEGF,⁴⁴ BCL-2, and Toll-like receptors that have the potential of synergistic responses.^{28,46} siRNA for the MDR-1 gene can increase drug treatment efficiency, as this gene's overexpression is correlated with drug resistance in GBM. Ultimately, a tailored treatment that is optimized for the GBM subtype, gene expression, and expected selection (depending on the chosen treatment) would most probably be highly effective for GBM patients.

Upon choosing the appropriate target genes, the HA-LNPs technology could be translated into medical practice. Treatment could thus be achieved

by applying repeated doses of HA-LNPs loaded with siRNAs using “frameless stereotactic apparatus”. This approach enables administration of NPs into a precise location of the tumor/tumor bed and allows accurate local targeting. Repeated administrations would be conducted in the operating room using frameless guided rapid single dose delivered each time. Alternatively, another option is frameless guided placement of a catheter in the operating room and then several hours' administration of the nanoparticles through this catheter under supervision in the neurosurgical intensive care unit. This procedure of convection-enhanced delivery (CED)⁴⁷ will allow continuous and slow administration of the medicine for up to 4 days in each round of treatment.

CONCLUSIONS

In this study, we have devised a novel strategy to target locally drug resistant glioma cells using lipid-based nanoparticles (LNPs) coated with hyaluronan

(HA), a CD44 natural ligand. These LNPs denoted HA-LNPs efficiently entrap siRNAs and deliver them to GBM cells in a specific manner while utilizing the CD44-HA interaction. HA-LNPs retain at the tumor vicinity even under shear flow and induce therapeutic gene silencing *in vitro* that cumulate in efficient cell death. In an orthotopic GBM mouse model, a robust (80%) reduction in the PLK1 mRNA level was observed in mice treated with siPLK1 delivered *via* HA-LNPs compared with other controls. This specific cell cycle inhibition by Polo-like Kinase 1 (PLK1) resulted in a dramatic prolongation of survival beyond any published report in this model. Our data suggest that this strategy may be applicable to clinical translation (using the microfluidic system) and imply that RNAi therapeutics could be effectively delivered in a localized manner. This strategy might aid as a novel tool to study gene expression of GBM within its microenvironment in the brain and ultimately might become a new therapeutic modality for GBM.

METHODS

Cell Lines. T98G, U251, and U87MG (WHO grade IV) human glioblastoma cell lines were used as model cells for GBM. The selected cell lines represent a spectrum of different genetic lesions. All cell lines were grown in monolayer and maintained in high-glucose (4.5 g/L) Dulbecco's modified Eagles's medium (DMEM) supplemented with 10% fetal bovine serum (FBS), 1% penicillin/streptomycin, and 2 mM L-glutamine (Biological Industries). Cells were incubated at 37 °C with 5% CO₂ and were subcultured twice weekly.

Flow Cytometry Analysis and Immunohistochemistry. Flow cytometry of cell surface CD44 antigens was performed as previously described.²² Briefly, Alexa Fluor 488-conjugated rat anti-human CD44 (clone 1M7) from Biolegend (San Diego, CA) or IgG2b isotype control was incubated with 0.5×10^6 GBM cells (0.25 µg per 10^6 cells) on ice for 30 min followed by washing with PBS. Data were acquired using FACSCalibur with CellQuest software (Becton Dickinson, Franklin Lakes, NJ). Data analysis was performed using the FlowJo software (Tree Star, Inc., Ashland, OR).

Eight paraffin blocks of GBM patients and a single gliosarcoma block were identified by examination of hematoxylin- and eosin-stained slides. From each tumor block, 4 µm thick sections were cut onto positive charged slides and used for IHC. The slides were warmed up to 60 °C for 1 h and after that processed to a fully automated protocol (Benchmark XT, Ventana Medical System, Inc., Tucson, AZ), and the related Ventana reagents were used according to standard manufacturer's instructions. Briefly, after sections were dewaxed and rehydrated, a CC1 standard Benchmark XT pretreatment (60 min) for antigen retrieval was selected (Ventana Medical Systems). Sections were then incubated 40 min with a prediluted mouse anti-human CD44 (08-0184 from Zymed, San Francisco, CA). Detection was performed with ultraView detection kit (Ventana Medical Systems) and counterstained with hematoxylin (4 min) (Ventana Medical Systems). After the run on the autostainer was completed, slides were dehydrated in 70% ethanol, 95% ethanol, and 100% ethanol for 10 s each ethanol. Before coverslipping, sections were cleared in xylene for 10 s and mounted with Entellan. Analysis score was based on CD44 scattering within the tumor site. This staining is semiquantitatively scored: + (positive), ++ (strongly positive), or +++ (very strongly positive).

Preparation of Lipid-Based Nanoparticles. Synthesis of Dlin-MC3-DMA: The ionizable lipid Dlin-MC3-DMA was synthesized according to a reported method.⁴⁸ The Dlin-MC3-DMA structure

was confirmed by NMR and ES-Mass spectra (see supplementary Figures 1 and 2, Supporting Information).

Preparation of amine-functionalized LNPs and siRNA entrapment: LNPs were prepared using microfluidic micro mixture (Precision NanoSystems, Vancouver, BC) as reported previously.³⁰ Briefly, one volume of lipid mixtures (Dlin-MC3-DMA, DSPC, Chol, DMG-PEG, and DSPE-PEG amine at 50:10:38:1.5:0.5 mol ratio, total lipid concentration 9.64 mM) were prepared in ethanol. Three volumes of siRNA (1:16 w/w siRNA to lipid) (Cy3-siLuci, siLuci, or siPLK1) containing acetate buffer solutions were mixed using a dual-syringe pump (Model S200, kD Scientific, Holliston, MA) to drive the solutions through the micromixer at a combined flow rate of 2 mL/min (0.5 mL/min for ethanol and 1.5 mL/min for aqueous buffer). The resultant mixture was dialyzed against PBS (pH 7.4) for 16 h to remove ethanol.

Luciferase-siRNA (siLuci) sequence was published⁴⁹ as well as PLK1-siRNA sequence (siPLK1).²⁶

Functionalization of LNPs with HA. HA modification of LNPs was achieved by amine coupling. First, carboxylic groups of HA (MW 5KDa, Lifecore Biomedical LLC, Chaska, MN) were activated by EDC/sulfo-NHS method as we previously reported.^{22,23} HA (0.3 mg, 5×10^5 mmol) was dissolved in water followed by the addition of EDC (0.2 mg, 10×10^5 mmol) and sulfo-NHS (0.3 mg, 10×10^5 mmol). The reaction mixture was stirred by a gentle shaker for 2 h followed by addition of amine-functionalized nanoparticles at pH 7.8 (containing 0.03 mg of PEG-amine, 1×10^5 mmol) and stirring continued for another 3 h. The reaction mixture was dialyzed against PBS (7.4) using a 12–14 kD cutoff membrane for 24 h to remove excess HA and EDC. HA was quantified as previously demonstrated.⁵⁰ The final HA/lipid ratio was typically 75 µg HA/µmole lipid as assayed by ³H-HA (ARC, Saint Louis, MI).

Size Distribution and ζ Potential Measurements. Particle size distribution and ζ potential measurements were determined by light scattering using a Malvern nano ZS zSizer (Malvern Instruments, Ltd., Worcestershire, UK). Size measurements were performed in HBS pH 7.4, and ζ potential measurements were performed in 0.01XHBS pH 7.4. Each experimental result was an average of at least six independent measurements.

Ultrastructure Analysis of HA-LNPs and LNPs-NH₂ by Electron Microscopy. Transmission Electron Microscopy (TEM) Analysis. LNPs were analyzed by transmission electron microscopy for their size and shape. A drop of aqueous solution containing LNPs (with or without HA) were placed on a carbon coated copper

grid and air-dried. The analysis was carried out on Joel 1200 EX (Japan) transmission electron microscopy.

Scanning electron microscopy (SEM): LNPs containing aqueous sample (with or without HA) were dried on silica wafers, and analysis was carried out on Quanta 200 FEG (USA) scanning electron microscopy.

siRNA Entrapment Efficiency. siRNA encapsulation efficiency was determined by the Quant-iT RiboGreen RNA assay (Life Technology) as previously described by us and others.^{31,51,52} Briefly, the entrapment efficiency was determined by comparing fluorescence of the RNA binding dye RiboGreen in the LNP-NH₂ and HA-LNPs samples, in the presence and absence of Triton X-100.⁵¹ In the absence of detergent, fluorescence can be measured from accessible (unentrapped) siRNA only, whereas, in the presence of the detergent, fluorescence is measured from total siRNA;⁵² thus, the % encapsulation is described by the following equation:

$$\% \text{ siRNA encapsulation} = [1 - (\text{free siRNA conc}/\text{total siRNA conc})] \times 100$$

Quantification of mRNA levels by QPCR. The mRNA levels of polio-like kinase 1 (PLK1 gene) in cells was quantified by real-time PCR. Seventy-two hours post-transfection (10 min under shear flow and additional 72 h under static conditions with full fresh media). Total RNA was isolated using the EzRNA RNA purification kit (Biological Industries, Beit Haemek, Israel), and 1 μ g of RNA from each sample was reverse transcribed into cDNA using the High Capacity cDNA Reverse Transcription Kit (Applied Biosystems, Foster City, CA), Quantification of cDNA (5 ng total) was performed on the step one Sequence Detection System (Applied Biosystems, Foster City, CA) using syber green (Applied Biosystems). GAPDH was chosen as a housekeeping gene.

For real time PCR the following primers were chosen:

Primers for PLK1:

forward - ACCAGCACGTCGTAGGATTC

reverse - CAAGCACAATTTGCCGTAGG

Primers for GAPDH:

forward - TCA GGG TTT CAC ATT TGG CA

reverse - GAG CAT GGA TCG GAA AAC CA

U87MG Orthotopic GBM Model Establishment. Cells were maintained in Dulbecco's modified Eagle's medium supplemented with 10% bovine serum and incubated at 37 °C in a humidified atmosphere containing 5% carbon dioxide/95% air. On the day of implantation, monolayer cell cultures were harvested using a 0.05% trypsin/ethylene diamine tetra acetic acid solution. Cells were counted, resuspended in 3 μ L of PBS. Five $\times 10^5$ U87MG cells were injected into each animal in a 3 μ L volume.

Animal Hosts. Four- to 6-week-old female nude mice (strain nu/nu), each weighing ~ 20 g, were used for this study. All procedures were performed in accordance with regulations of the Animal Care and Use Committee of the Sheba Medical Center. The mice were housed in groups of five in cages within a standardized barrier facility and maintained on a 12-h day/night cycle at 23 °C. Animals were given free access to laboratory chow and water. All instruments were sterilized before the procedure, and sterile small-animal surgical techniques were used. The mice were allowed to feed until the time of surgery. Animals were anesthetized by intraperitoneal injection of ketamine/xylazine solution (200 mg ketamine and 20 mg xylazine in 17 mL of saline) at a dosage of 0.15 mg/10 g body weight.

Identification of Implantation Site. The animal's head was stabilized manually by holding it with one finger behind the interaural line. The skin was prepared with povidone iodine solution, and then a 2- to 3-mm-long incision was made just to the right of midline and anterior to the interaural line so that the coronal and sagittal sutures could be identified; the bregma was located. The entry site was marked at a point 2.5 mm lateral and 1 mm anterior to the bregma. This point was chosen because it is located directly above the caudate nucleus, which has been shown to be a highly reliable intracranial site for tumor engraftment.

Drill Hole Placement. Using a small hand-controlled twist drill that is 1 mm in diameter a drill hole was made in the

animal's skull at the entry point. The drill bit penetrates the dura and thereby opens it.

Cell Injection with Hamilton Syringe. The 3- μ L cell suspension was drawn up into the cuff of the 26-gauge needle of a Hamilton syringe. Using a stereotactic apparatus, the needle of the Hamilton syringe was slowly lowered into the central skull hole made by the twist drill. Based on the entry point and the depth of needle penetration, it is certain that the cells are injected into the caudate nucleus. The cell suspension was slowly injected (typically over 5 min) into the mouse's brain. After the entire volume of the cell suspension was injected, the needle was manually removed. A suture was placed to close the scalp. The mice were kept warm until they recover from anesthesia and were allowed to move around freely until the time of intratumoral injection of the therapeutic interventions. In the interim the injected tumor cells proliferate and establish themselves as intraparenchymal xenografts. The technique of intratumoral injection mimics the technique of tumor cell implantation, except that HA-LNPs were delivered into the established xenograft in 4 doses of 3 μ L each. The first doses were given at days 7 and 9 and the next doses were given at days 20 and 22. Mice were monitored for global toxicity changes including changes in body weight that were not observed for the entire period of the experiment.

Assessing PLK1 Knockdown in Vivo. In order to identify the U87MG cells *in vivo* upon single Cy3-siRNA administration (entrapped within HA-LNPs), mice were sacrificed 3, 6, and 24 h post-administration. A single cell suspension from brain tissue was performed. Neural tissues were dissociated to single-cell suspension by enzymatic degradation using the GentleMACS dissociator and neural tissue dissociation kit (Miltenyi Biotech), according to the company's protocol. Briefly, mice were perfused with either HBSS or PBS, and brains were removed and weighed in order to adjust the buffers and enzyme mix to the amount of tissue. A prewarmed enzyme mix was added to the tissue and incubated with agitation at 37 °C. The tissue was mechanically dissociated, and the suspension was applied to a 70 μ m strainer. Myelin was removed using Myelin Removal Beads II (Miltenyi Biotech) as it can interfere with flow cytometric analysis. Cells were processed immediately and stained with antihuman CD44v6-FITC (non-cross-reactive with mice, clone MCA1730F, Bio-Rad) in order to identify the U87MG cells. Cells were incubated on ice for 30 min, washed twice, and subjected to FACS sorting using FACSAria III (BD). Sorted cells were moved directly into an EzRNA RNA purification kit (Biological Industries, Beit Haemek, Israel) and analyzed for PLK1 mRNA levels using QPCR as detailed above.

Statistical Analysis. Differences between two means were tested using an unpaired, two-sided Student's *t*-test. Differences between treatment groups were evaluated by one-way ANOVA test of SPSS software. Kaplan–Meier survival analysis was performed with a GraphPad Prism version 5.0b.

Conflict of Interest: The authors declare the following competing financial interest: D.P. has financial interest in Quiet Therapeutics. The rest of the authors declare no competing financial interest.

Supporting Information Available: NMR spectrum of Dlin-MC3-DMA, ESI-MS of Dlin-MC3-DMA, and cell survival assay of U87MG cells. Cytokine induction in primary CD11b⁺ cells assays. This material is available free of charge via the Internet at <http://pubs.acs.org>.

Acknowledgment. Z.R.C. thanks the Israel Cancer Association (Grant No. 20130092) for partial support of this work. S.R. thanks Tel Aviv University Center for Nanoscience and Nanotechnology for an excellence postdoctoral fellowship. This work was supported in part by grants from the MOST – Tashtiyot (Grant No. 880011), the Israeli Centre of Research Excellence (I-CORE), Gene Regulation in Complex Human Disease, Center No. 41/11; FTA: Nanomedicine for Personalized Therapeutics, The Leona M. and Harry B. Helmsley Nanotechnology Research Fund, and the Susan and Len Mark Nanotechnology Research Fund for solid tumors awarded to D.P.

REFERENCES AND NOTES

- Lacroix, M.; Abi-Said, D.; Fourney, D. R.; Gokaslan, Z. L.; Shi, W.; DeMonte, F.; Lang, F. F.; McCutcheon, I. E.; Hassenbusch, S. J.; Holland, E.; et al. A Multivariate Analysis of 416 Patients with Glioblastoma Multiforme: Prognosis, Extent of Resection, and Survival. *J. Neurosurg.* **2001**, *95*, 190–198.
- Saito, N.; Fu, J.; Zheng, S.; Yao, J.; Wang, S.; Liu, D. D.; Yuan, Y.; Sulman, E. P.; Lang, F. F.; Colman, H.; et al. A High Notch Pathway Activation Predicts Response to Gamma Secretase Inhibitors in Proneural Subtype of Glioma Tumor-Initiating Cells. *Stem Cells* **2014**, *32*, 301–312.
- Berghoff, A. S.; Kiesel, B.; Widhalm, G.; Rajky, O.; Ricken, G.; Wohrer, A.; Dieckmann, K.; Filipits, M.; Brandstetter, A.; Weller, M., et al. Programmed Death Ligand 1 Expression and Tumor-Infiltrating Lymphocytes in Glioblastoma. *Neuro Oncol.* **2014**; pii: nou307.
- Stummer, W.; Pichlmeier, U.; Meinel, T.; Wiestler, O. D.; Zanella, F.; Reulen, H. J.; Group, A. L.-G. S. Fluorescence-Guided Surgery with 5-Aminolevulinic Acid for Resection of Malignant Glioma: A Randomised Controlled Multicentre Phase III Trial. *Lancet Oncol.* **2006**, *7*, 392–401.
- Senft, C.; Bink, A.; Franz, K.; Vatter, H.; Gasser, T.; Seifert, V. Intraoperative MRI Guidance and Extent of Resection in Glioma Surgery: A Randomised, Controlled Trial. *Lancet Oncol.* **2011**, *12*, 997–1003.
- Westphal, M.; Yla-Herttuala, S.; Martin, J.; Warnke, P.; Menei, P.; Eckland, D.; Kinley, J.; Kay, R.; Ram, Z.; Group, A. S. Adenovirus-Mediated Gene Therapy with Sitimagene Ceradenovec Followed by Intravenous Ganciclovir for Patients with Operable High-Grade Glioma (ASPECT): A Randomised, Open-Label, Phase 3 Trial. *Lancet Oncol.* **2013**, *14*, 823–833.
- Sampson, J. H.; Archer, G.; Pedain, C.; Wembacher-Schroder, E.; Westphal, M.; Kunwar, S.; Vogelbaum, M. A.; Coan, A.; Herndon, J. E.; Raghavan, R.; et al. Poor Drug Distribution as a Possible Explanation for the Results of the PRECISE Trial. *J. Neurosurg.* **2010**, *113*, 301–309.
- Peer, D.; Karp, J. M.; Hong, S.; Farokhzad, O. C.; Margalit, R.; Langer, R. Nanocarriers as an Emerging Platform for Cancer Therapy. *Nat. Nanotechnol.* **2007**, *2*, 751–760.
- Lynch, I.; Dawson, K. A.; Linse, S. Detecting Cryptic Epitopes Created by Nanoparticles. *Science's STKE* **2006**, pe14.
- Hernandez-Pedro, N. Y.; Rangel-Lopez, E.; Magana-Maldonado, R.; de la Cruz, V. P.; del Angel, A. S.; Pineda, B.; Sotelo, J. Application of Nanoparticles on Diagnosis and Therapy in Gliomas. *BioMed. Res. Int.* **2013**, 351031.
- Chen, H.; Qin, Y.; Zhang, Q.; Jiang, W.; Tang, L.; Liu, J.; He, Q. Lactoferrin Modified Doxorubicin-Loaded Procationic Liposomes for the Treatment of Gliomas. *Eur. J. Pharma Sci.* **2011**, *44*, 164–173.
- Gong, W.; Wang, Z.; Liu, N.; Lin, W.; Wang, X.; Xu, D.; Liu, H.; Zeng, C.; Xie, X.; Mei, X.; et al. Improving Efficiency of Adriamycin Crossing Blood Brain Barrier by Combination of Thermosensitive Liposomes and Hyperthermia. *Biol. Pharm. Bull.* **2011**, *34*, 1058–1064.
- Qin, Y.; Chen, H.; Zhang, Q.; Wang, X.; Yuan, W.; Kuai, R.; Tang, J.; Zhang, L.; Zhang, Z.; Zhang, Q.; et al. Liposome Formulated with TAT-Modified Cholesterol for Improving Brain Delivery and Therapeutic Efficacy on Brain Glioma in Animals. *Int. J. Pharm.* **2011**, *420*, 304–312.
- Tezcan, G.; Tunca, B.; Bekar, A.; Budak, F.; Sahin, S.; Cecener, G.; Egeli, U.; Taskapilioglu, M. O.; Kocaali, H.; Tolunay, S. et al. Olea Europaea Leaf Extract Improves the Treatment Response of GBM Stem Cells by Modulating miRNA Expression. *Am. J. Cancer Res.* **2014**, *4*, 572–590.
- Hong, X. Y.; Wang, J.; Li, Z. AGR2 Expression is Regulated by HIF-1 and Contributes to Growth and Angiogenesis of Glioblastoma. *Cell Biochem. Biophys.* **2013**, *67*, 1487–1495.
- Platt, V. M.; Szoka, F. C., Jr. Anticancer Therapeutics: Targeting Macromolecules and Nanocarriers to Hyaluronan or CD44, A Hyaluronan Receptor. *Mol. Pharmaceutics* **2008**, *5*, 474–486.
- Eliaz, R. E.; Szoka, F. C., Jr. Liposome-Encapsulated Doxorubicin Targeted to CD44: A Strategy to Kill CD44-Overexpressing Tumor Cells. *Cancer Res.* **2001**, *61*, 2592–2601.
- Peer, D.; Margalit, R. Tumor-Targeted Hyaluronan Nanoliposomes Increase the Antitumor Activity of Liposomal Doxorubicin in Syngeneic and Human Xenograft Mouse Tumor Models. *Neoplasia* **2004**, *6*, 343–353.
- Peer, D.; Margalit, R. Loading Mitomycin C Inside Long Circulating Hyaluronan Targeted Nano-Liposomes Increases its Antitumor Activity in Three Mice Tumor Models. *Int. J. Cancer* **2004**, *108*, 780–789.
- Poon, Z.; Lee, J. B.; Morton, S. W.; Hammond, P. T. Controlling *In Vivo* Stability and Biodistribution in Electrostatically Assembled Nanoparticles for Systemic Delivery. *Nano Lett.* **2011**, *11*, 2096–2103.
- Rivkin, I.; Cohen, K.; Koffler, J.; Melikhov, D.; Peer, D.; Margalit, R. Paclitaxel-Clusters Coated with Hyaluronan as Selective Tumor-Targeted Nanovectors. *Biomaterials* **2010**, *31*, 7106–7114.
- Cohen, K.; Emmanuel, R.; Kisin-Finifer, E.; Shabat, D.; Peer, D. Modulation of Drug Resistance in Ovarian Adenocarcinoma using Chemotherapy Entrapped in Hyaluronan-Grafted Nanoparticle Clusters. *ACS Nano* **2014**, *8*, 2183–2195.
- Mizrahy, S.; Goldsmith, M.; Leviatan-Ben-Arye, S.; Kisin-Finifer, E.; Redy, O.; Srinivasan, S.; Shabat, D.; Godin, B.; Peer, D. Tumor Targeting Profiling of Hyaluronan-Coated Lipid Based-Nanoparticles. *Nanoscale* **2014**, *6*, 3742–3752.
- Mizrahy, S.; Raz, S. R.; Hasgaard, M.; Liu, H.; Soffer-Tsur, N.; Cohen, K.; Dvash, R.; Landsman-Milo, D.; Bremer, M. G.; Moghimi, S. M.; et al. Hyaluronan-Coated Nanoparticles: The Influence of the Molecular Weight on CD44-Hyaluronan Interactions and on the Immune Response. *J. Controlled Release* **2011**, *156*, 231–238.
- Bachar, G.; Cohen, K.; Hod, R.; Feinmesser, R.; Mizrahi, A.; Shpitzer, T.; Katz, O.; Peer, D. Hyaluronan-Grafted Particle Clusters Loaded with Mitomycin C as Selective Nanovectors for Primary Head and Neck Cancers. *Biomaterials* **2011**, *32*, 4840–4848.
- Yao, Y. D.; Sun, T. M.; Huang, S. Y.; Dou, S.; Lin, L.; Chen, J. N.; Ruan, J. B.; Mao, C. Q.; Yu, F. Y.; Zeng, M. S.; et al. Targeted Delivery of PLK1-siRNA by ScFv Suppresses Her2+ Breast Cancer Growth and Metastasis. *Sci. Transl. Med.* **2012**, *4*, 130ra48.
- Cheng, M. W.; Wang, B. C.; Weng, Z. Q.; Zhu, X. W. Clinicopathological Significance of Polo-Like Kinase 1 (PLK1) Expression in Human Malignant Glioma. *Acta Histochem.* **2012**, *114*, 503–509.
- Signore, M.; Pelacchi, F.; di Martino, S.; Runci, D.; Biffoni, M.; Giannetti, S.; Morgante, L.; De Majo, M.; Petricoin, E. F.; Stancato, L.; et al. Combined PDK1 and CHK1 Inhibition is Required to Kill Glioblastoma Stem-Like Cells *In Vitro* and *In Vivo*. *Cell Death Dis.* **2014**, *5*, e1223.
- Pyko, I. V.; Nakada, M.; Sabit, H.; Teng, L.; Furuyama, N.; Hayashi, Y.; Kawakami, K.; Minamoto, T.; Fedulau, A. S.; Hamada, J. Glycogen Synthase Kinase 3Beta Inhibition Sensitizes Human Glioblastoma Cells to Temozolomide by Affecting O6-Methylguanine DNA Methyltransferase Promoter Methylation via c-Myc Signaling. *Carcinogenesis* **2013**, *34*, 2206–2217.
- Rungta, R. L.; Choi, H. B.; Lin, P. J.; Ko, R. W.; Ashby, D.; Nair, J.; Manoharan, M.; Cullis, P. R.; Macvicar, B. A. Lipid Nanoparticle Delivery of siRNA to Silence Neuronal Gene Expression in the Brain. *Mol. Ther. Nucleic Acids* **2013**, *2*, e136.
- Peer, D.; Park, E. J.; Morishita, Y.; Carman, C. V.; Shimaoka, M. Systemic Leukocyte-Directed siRNA Delivery Revealing Cyclin D1 as an Anti-Inflammatory Target. *Science* **2008**, *319*, 627–630.
- Mizrahy, S.; Peer, D. Polysaccharides as Building Blocks for Nanotherapeutics. *Chem. Soc. Rev.* **2012**, *41*, 2623–2640.
- Ganoth, A.; Merimi, K. C.; Peer, D. Overcoming Multidrug Resistance with Nanomedicines. *Expert Opin. Drug Deliv.* **2014**, 1–16.
- Drinberg, V.; Bitcover, R.; Rajchenbach, W.; Peer, D. Modulating Cancer Multidrug Resistance by Sertraline in Combination with a Nanomedicine. *Cancer Lett.* **2014**, *354*, 290–298.

35. Shulman, Z.; Alon, R. Chapter 14. Real-Time *In Vitro* Assays for Studying the Role of Chemokines in Lymphocyte Transendothelial Migration Under Physiologic Flow Conditions. *Methods Enzymol.* **2009**, *461*, 311–332.
36. Kuroda, J.; Kuratsu, J.; Yasunaga, M.; Koga, Y.; Kenmotsu, H.; Sugino, T.; Matsumura, Y. Antitumor Effect Of NK012, A 7-Ethyl-10-Hydroxycamptothecin-Incorporating Polymeric Micelle, on U87MG Orthotopic Glioblastoma in Mice Compared with Irinotecan Hydrochloride in Combination with Bevacizumab. *Clin. Cancer Res.* **2010**, *16*, 521–529.
37. Li, C.; Zhou, Y.; Peng, X.; Du, L.; Tian, H.; Yang, G.; Niu, J.; Wu, W. Sulforaphane Inhibits Invasion Via Activating ERK1/2 Signaling in Human Glioblastoma U87MG and U373MG Cells. *PLoS One* **2014**, *9*, e90520.
38. Kumar, P.; Wu, H.; McBride, J. L.; Jung, K. E.; Kim, M. H.; Davidson, B. L.; Lee, S. K.; Shankar, P.; Manjunath, N. Transvascular Delivery of Small Interfering RNA to the Central Nervous System. *Nature* **2007**, *448*, 39–43.
39. Sakurai, Y.; Hatakeyama, H.; Akita, H.; Harashima, H. Improvement of Doxorubicin Efficacy Using Liposomal Anti-Polo-Like Kinase 1 siRNA in Human Renal Cell Carcinomas. *Mol. Pharmaceutics* **2014**, *11*, 2713–2719.
40. Cho, D. Y.; Lin, S. Z.; Yang, W. K.; Lee, H. C.; Hsu, D. M.; Lin, H. L.; Chen, C. C.; Liu, C. L.; Lee, W. Y.; Ho, L. H. Targeting Cancer Stem Cells for Treatment of Glioblastoma Multiforme. *Cell Transplant* **2013**, *22*, 731–739.
41. Denysenko, T.; Gennero, L.; Roos, M. A.; Melcarne, A.; Juenemann, C.; Faccani, G.; Morra, I.; Cavallo, G.; Reguzzi, S.; Pescarmona, G.; et al. Glioblastoma Cancer Stem Cells: Heterogeneity, Microenvironment and Related Therapeutic Strategies. *Cell Biochem. Funct.* **2010**, *28*, 343–351.
42. Phillips, J. J. Novel Therapeutic Targets in the Brain Tumor Microenvironment. *Oncotarget* **2012**, *3*, 568–575.
43. Wainwright, D. A.; Chang, A. L.; Dey, M.; Balyasnikova, I. V.; Kim, C. K.; Tobias, A.; Cheng, Y.; Kim, J. W.; Qiao, J.; Zhang, L.; et al. Durable Therapeutic Efficacy Utilizing Combinatorial Blockade against IDO, CTLA-4, and PD-L1 in Mice with Brain Tumors. *Clin. Cancer Res.* **2014**, *20*, 5290–5301.
44. Yi, N.; Oh, B.; Kim, H. A.; Lee, M. Combined Delivery of BCNU and VEGF siRNA Using Amphiphilic Peptides for Glioblastoma. *J. Drug Target* **2014**, *22*, 156–164.
45. Low, S. Y.; Ho, Y. K.; Too, H. P.; Yap, C. T.; Ng, W. H. MicroRNA as Potential Modulators in Chemoresistant High-Grade Gliomas. *J. Clin. Neurosci.* **2014**, *21*, 395–400.
46. Karpel-Massler, G.; Westhoff, M. A.; Zhou, S.; Nonnenmacher, L.; Dwucet, A.; Kast, R. E.; Bachem, M. G.; Wirtz, C. R.; Debatin, K. M.; Halatsch, M. E. Combined Inhibition of HER1/EGFR and RAC1 Results in a Synergistic Antiproliferative Effect on Established and Primary Cultured Human Glioblastoma Cells. *Mol. Cancer Ther.* **2013**, *12*, 1783–1795.
47. Goldberg, L.; Ocherashvilli, A.; Daniels, D.; Last, D.; Cohen, Z. R.; Tamar, G.; Kloog, Y.; Mardor, Y. Salirasib (Farnesyl Thiosalicylic Acid) for Brain Tumor Treatment: A Convection-Enhanced Drug Delivery Study in Rats. *Mol. Cancer Ther.* **2008**, *7*, 3609–3616.
48. Jayaraman, M.; Ansell, S. M.; Mui, B. L.; Tam, Y. K.; Chen, J.; Du, X.; Butler, D.; Eltepu, L.; Matsuda, S.; Narayanannair, J. K.; et al. Maximizing The Potency of siRNA Lipid Nanoparticles for Hepatic Gene Silencing *In Vivo*. *Angew. Chem., Int. Ed.* **2012**, *51*, 8529–8533.
49. Weinstein, S.; Emmanuel, R.; Jacobi, A. M.; Abraham, A.; Behlke, M. A.; Sprague, A. G.; Novobrantseva, T. I.; Nagler, A.; Peer, D. RNA Inhibition Highlights Cyclin D1 as a Potential Therapeutic Target for Mantle Cell Lymphoma. *PLoS One* **2012**, *7*, e43343.
50. Landesman-Milo, D.; Goldsmith, M.; Leviatan Ben-Arye, S.; Witenberg, B.; Brown, E.; Leibovitch, S.; Azriel, S.; Tabak, S.; Morad, V.; Peer, D. Hyaluronan Grafted Lipid-Based Nanoparticles as Rnai Carriers for Cancer Cells. *Cancer Lett.* **2013**, *334*, 221–227.
51. Morrissey, D. V.; Lockridge, J. A.; Shaw, L.; Blanchard, K.; Jensen, K.; Breen, W.; Hartsough, K.; Machermer, L.; Radka, S.; Jadhav, V.; et al. Potent and Persistent *In Vivo* Anti-HBV Activity of Chemically Modified siRNAs. *Nat. Biotechnol.* **2005**, *23*, 1002–1007.
52. Leuschner, F.; Dutta, P.; Gorbатов, R.; Novobrantseva, T. I.; Donahoe, J. S.; Courties, G.; Lee, K. M.; Kim, J. I.; Markmann, J. F.; Marinelli, B.; et al. Therapeutic siRNA Silencing in Inflammatory Monocytes in Mice. *Nat. Biotechnol.* **2011**, *29*, 1005–1010.